SERS

DOI: 10.1002/smll.200800301

Nanoparticle-Decorated Nanocanals for Surface-Enhanced Raman Scattering**

*Hyunhyub Ko and Vladimir V. Tsukruk**

The surface-enhanced Raman scattering (SERS) effect is considered important for fast detection of characteristic "fingerprint" signatures of analytes.[1] In the SERS effect, a substantial Raman enhancement arises on localized spots ("hot spots") in metallic nanostructures owing to strong local electromagnetic fields associated with the surface plasmon resonances of metal nanostructures.[2–4] SERS on colloidal metal aggregates and nanowires[5–7] and Raman resonances have been utilized for trace detection of explosives,[8,9] chemical and biological warfare agents,[10] internal mechanical stress,[11–14] distribution and stress of carbon nanotubes,[15,16] and toxic environmental pollutants.[17] However, an outstanding challenge of SERS-based detection is the lack of robust and facile fabrication routines for SERS substrates with considerable enhancements. Traditionally, electrochemically roughened metal surfaces,[18] colloids,[19] island films,[20,21] nanowires,[22] periodic arrays,[23,24] and self-assembled nanoparticles[25,26] are employed as SERS substrates (for a recent review, see Reference [27]). However, the long-term stability of aggregated nanoparticles is the main obstacle for assembled structures, and the fabrication of complex surface structures (e.g. with microfabrication) is labor- and cost-demanding and sometimes impossible to extend to large dimensions. Moreover, the sensitivity of simple 2D SERS substrates remains modest owing to a limited number of hot spots (usually below 10^5).[1,28]

To increase the sensitivity of SERS substrates, 3D porous structures have been suggested as active SERS substrates with the advantage of having a large surface area available for the formation of hot spots and the adsorption of target analytes. Consequently, 3D SERS substrates have been fabricated by depositing Au or Ag films on porous silicon,[29] GaN,[30] and filter paper.[31] Alternatively, deposition of metal nanoparticles on the porous aluminum membranes,[32,33] colloidal crystal templates,[34,35] or microwires[36] have been exploited. For instance, nanopores in gold films have been proven to show enhanced Raman scattering owing to an intense electromagnetic field generated by the surface plasmons.[37,38] However, most of these studies have not fully utilized the advantages of 3D structures for SERS effects, mainly because of limited light propagation through porous materials owing to significant scattering and adsorption on pore walls and a significant fraction of closed pores, which do not participate in SERS enhancement.[39] Moreover, even though significant enhancements have been claimed for porous SERS substrates (up to 10^8 in some cases),[29,30] these effects have been only demonstrated for organic dyes with intense resonant Raman peaks and not for conventional molecules with modest Raman scattering.

Herein we introduce nanocanal arrays composed of uniformly aligned vertical cylindrical pores with inner walls decorated with gold nanoparticles as robust and cost-efficient SERS substrates with significant SERS enhancement. These substrates are successfully employed in this case for the detection of trace amounts of 2,4-dinitrotoluene (2,4-DNT), a model nitroaromatic compound for TNT-based plastic explosives with modest Raman cross-section. This class of compound is usually not detected by conventional Raman measurements.[40] The use of porous alumina membranes as SERS substrates is especially promising considering the efficient interaction of light with the inner walls of the cylindrical pores as well as their optical transparency with minimal light absorption and scattering.[41,42] In addition, their easy fabrication and very modest cost (at least an order of magnitude lower than commercially available microfabricated substrates) combined with large area (up to 5 centimeters in diameter) are attractive practical features for sensing elements.[43]

Figure 1 illustrates the fabrication procedure for nanocanal arrays decorated with gold nanoparticles (see Experimental Section for details). A representative cross-sectional scanning electron microscopy (SEM) image of decorated nanocanals (240-nm diameter) within porous alumina membranes shows that most of the gold nanoparticles (32 nm) are immobilized in an isolated state with occasional aggregated clusters inside the pore walls modified with poly(diallyldimethylammonium chloride) (PDDA) polyelectrolyte (Figure 2a). The immobilized nanoparticles inside the pores can be also observed from the SEM image obtained with a tilt angle (Figure 2b). Energy-dispersive spectroscopy (EDS) confirmed the presence of gold nanoparticles immobilized inside the nanocanals (Figure 2a). Few nanoparticles were observed on the outer surfaces of the nanohole arrays, in contrast to the nanoparticle immobilization inside the pore walls. Immobilization inside the PDDA-modified pores can be related to partial replacement of the cetyltrimethylammonium bromide (CTAB) ligand.

The PDDA polyelectrolyte used in this case can act as a selective coating to increase the adsorption of DNT on the gold nanoparticle surface owing to the interactions between the electron-donating amine-groups in PDDA and the electron-deficient NO_2 groups of 2,4-DNT.[44] A control Raman experiment of 2,4-DNT adsorbed on a PDDA-modified porous membrane (case 1, Figure 3b) provides no measurable signals (spectrum 1, Figure 3c). In this study, we used a near-IR laser (785 nm) as the excitation source because its wavelength is close to the expected coupled surface plasmon resonance[45] and because of its higher transmission through the aluminum membrane. Notably, our attempts to use 514-nm light showed low intensity owing to the high absorption, similar to cases reported in the literature.[46]

[*] Prof. V. V. Tsukruk, Dr. H. Ko
School of Materials Science and Engineering
Georgia Institute of Technology
Atlanta, GA 30332 (USA)
E-mail: vladimir@mse.gatech.edu

[**] We thank R. Gunawidjaja, C. Jiang, and Y.-H. Lee for discussions and technical assistance and M. Srinivasarao for use of a Raman instrument. This work was supported by the Army Research Office and Agiltron.

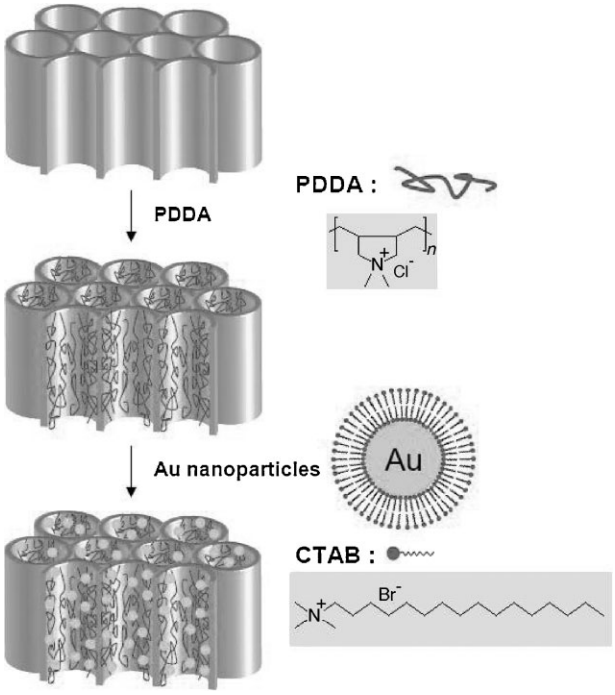

Figure 1. Fabrication procedures for nanohole arrays decorated with gold nanoparticles. Porous alumina membranes are functionalized with positively charged amine groups by modification with PDDA. CTAB-capped gold colloids are passed through the modified porous membranes, resulting in Au nanoparticle immobilization.

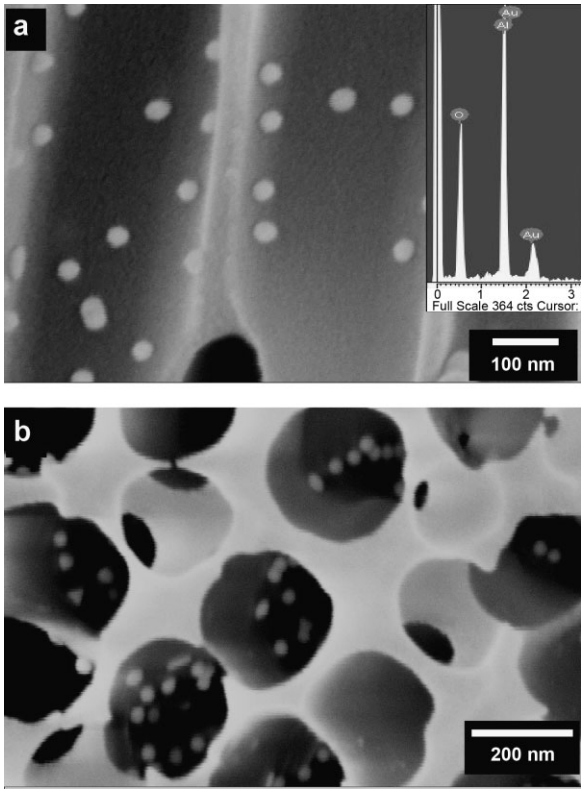

Figure 2. a) Cross-sectional and b) angle-view SEM images of porous alumina membranes decorated with Au nanoparticles. The inset in (a) shows the EDS spectrum, which indicates the presence of Au inside the pore walls.

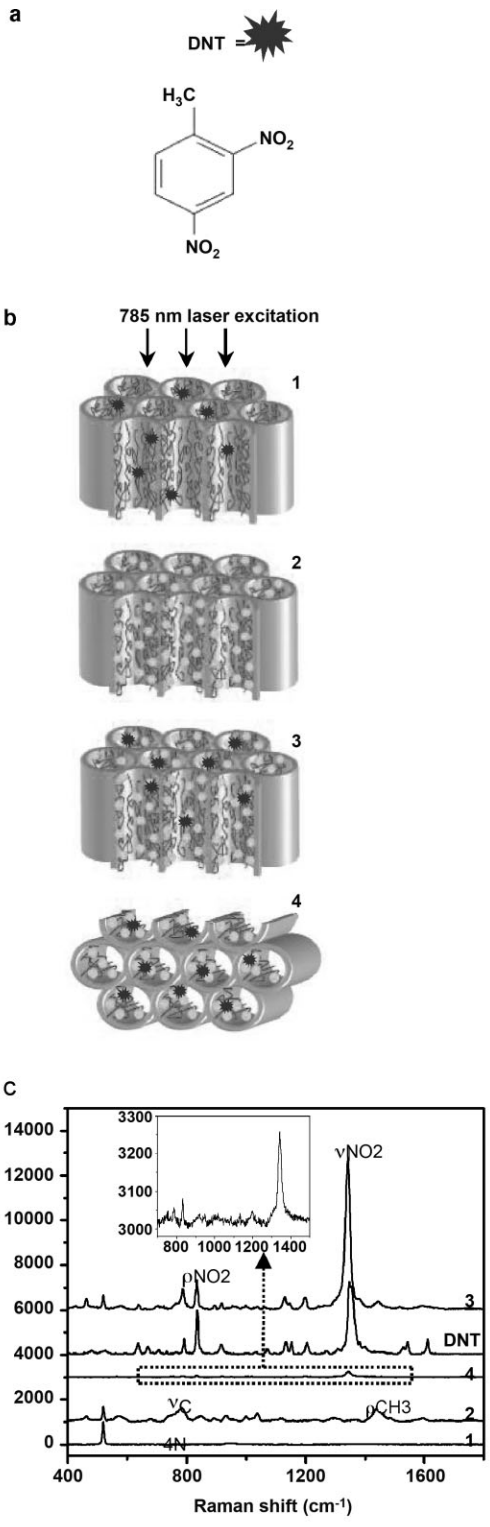

Figure 3. a) Chemical structure of 2,4-DNT. b) Schematic representation of the Raman measurement of 2,4-DNT with different configurations and light incidences to the SERS substrates. The excitation light incidence is parallel (1,2,3) and perpendicular (4) to the pore axes. c) The Raman spectrum of DNT powder and 1000 ppm 2,4-DNT on each substrate shown schematically in (b). The spectrum 4 is shown clearly in the inset. A solution of 2,4-DNT in ethanol (10 μL) was drop-evaporated on substrates with areas of 1 cm^2. The Raman spectra were background corrected for clarity.

A strong peak at 520 cm^{-1} for silicon arises from the supporting silicon substrate, indicating that the excitation light passes through whole membrane (60 μm thick) and reflects back, traveling through the vertically aligned nanocanals (Figure 1c). The addition of gold nanoparticles activates the SERS effect for the PDDA layer (case 2, Figure 3b), revealing their characteristic Raman signatures: C_4N stretching modes (ν_{C4N}) at 783 cm^{-1} and CH_3 asymmetric bending modes (ρ_{CH3}) at 1444 cm^{-1} (spectrum 2, Figure 3c).[47]

Deposition of 2,4-DNT analyte by means of drop-casting (case 3, Figure 3b) dramatically changes the SERS spectra, with two intense peaks corresponding to two representative 2,4-DNT vibration modes: NO_2 out-of-plane bending modes (ρ_{NO2}) at 834 cm^{-1} and NO_2 stretching modes (ν_{NO2}) at 1342 cm^{-1} (spectrum 3, Figure 3c, see also Raman spectrum from bulk DNT in Figure 3c for comparison).[8] Moreover, the silicon Raman peak is still strong, which indicates the reflection of the laser beam after passing through the modified nanocanals. Indeed, if we consider the initial diameter of the nanocanals to be 240 nm and the thickness of the polyelectrolyte layer with immobilized nanoparticles on both walls to be less than 70 nm, we can conclude that the light passes through the vertical nanocanals without much absorption. The critical importance of the ability of the laser beam to pass through the whole membrane is illustrated by the tremendous reduction of the Raman signal when the light is directed in the transversal direction (case 4, Figure 3b). Only a very weak ν_{NO2} signal at 1342 cm^{-1} is observed under this orientation, and the band for silicon disappears completely (spectrum 4, Figure 3c).

The much stronger Raman enhancement from the vertically oriented nanocanals (case 3, Figure 3b) allows trace level detection of DNT (Figure 4a). The Raman spectrum of a solution of 2,4-DNT (100 ppb; 10 μL) evaporated on the SERS substrate clearly shows NO_2 stretching modes of DNT at 1342 cm^{-1}, distinctive from several PDDA-related Raman peaks such as ν_{C4N} at 783 cm^{-1} and ρ_{CH3} at 1444 cm^{-1}. The minimum detection limit under our current measurement conditions (20-s acquisition time, 20-mW laser power, 10 μL of DNT solution uniformly drop-evaporated on 1-cm^2 substrates) estimated from a signal-to-noise ratio (S/N ratio of 15) for this spectrum can be as low as 10 fg. This detection limit is two orders of magnitude better than the best detection amount of 1 pg of 2,4-DNT reported for highly oriented silver nanowire films[9] and roughened gold substrates.[48]

The Raman enhancement factor (*EF*) was estimated by using a reference sample without SERS contribution: $EF = I_{SERS}/I_{Ref} \times$ [reference]/[sample],[49,50] where I_{SERS} and I_{Ref} are the Raman intensities of the spectra and [SERS] and [reference] are the concentrations of the target molecules in the SERS and reference samples, respectively. By comparing the peak intensity of the characteristic band at 1342 cm^{-1} with a normal Raman peak of a reference 2,4-DNT film of known thickness, we can estimate the SERS enhancement factor to be about 1.1×10^6. This unexpectedly high SERS enhancement relative to those of 2D substrates with individual nanoparticles cannot be caused by the trivial increase in specific surface area. The excessive Raman enhancement can, at first glance, be associated with the effect of resonance coupling between neighboring nanoparticles localized on the inner walls of the nanocanals (hot spots). However, most of the gold nanoparticles on the inner walls are present in the isolated form, with only a few aggregates observed occasionally (Figure 2). Moreover, the estimation of the average distance between far-placed gold nanoparticles does not support this suggestion. In fact, the value obtained is close to 100 nm or a distance/diameter ratio *d*/*D* of about 3, well above the value suggested for maximum enhancement.[51–53] Finally, analysis of the SEM images showed that very few nanoparticle aggregates, which could contain hot spots, are present in our substrates under the current preparation conditions. The increase in the nanoparticle density and their controlled aggregation are difficult tasks and will require additional studies.

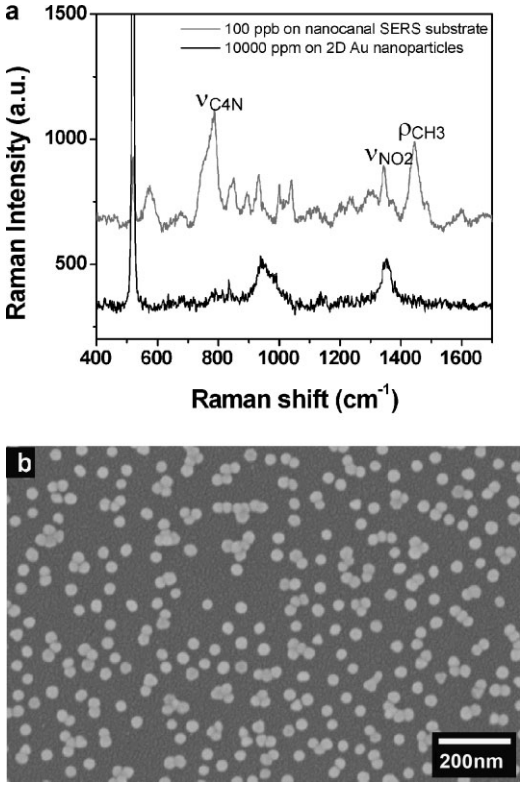

Figure 4. a) Raman spectra of 100 ppb 2,4-DNT drop-evaporated on the SERS substrates with PDDA/Au nanoparticles/PDDA/PAM on top of silicon substrates and control Raman spectra of 10000 ppm 2,4-DNT on a 2D substrate. b) SEM image of a 2D substrate of gold nanoparticles with few aggregates.

A control Raman study on a 2D gold nanoparticle array with similar nanoparticle surface density was conducted to evaluate this contribution (Figure 4b). The Raman spectrum of a solution of 2,4-DNT (10000 ppm) showed only weak and broad NO_2 stretching modes of DNT at 1342 cm^{-1} (Figure 4a). From the Raman peak intensities, we estimate that the SERS enhancement of this 2D substrate with relatively low concentration and very few aggregates of gold nanoparticles was only about 10, owing to a rare presence of hot spots. However, a 3D nanocanal array with an identical concentration of predominantly isolated gold nanoparticles led to an enhancement about five orders of magnitude higher than that

observed on a gold nanoparticle monolayer with identical surface densities of gold nanoparticles.

Considering the geometry of the nanocanal arrays and the minor contributions from specific surface area and traditional hot spots, we suggest that the optical waveguide effect of vertical alumina-pore arrays with excited evanescent electrical field is responsible for the observed enhancement of Raman scattering. The propagating light can be trapped inside the alumina nanowalls with total internal reflection caused by the high refractive index difference between alumina ($n \approx 1.6$) and the air/polymer monolayer ($n = 1$ and 1.5). This multiple reflection can lead to a higher photon density of states at the alumina–inner coating interface,[54] resulting in increased probability of Raman scattering by interaction of the evanescent field with the gold nanoparticles tethered to the inner surface of the nanocanals. This Raman enhancement resembles optical microcavities with cylindrical resonators[55,56] and nanoribbons.[57] In these systems, additional optical gains were acquired through microcavity resonances. However, the waveguide effect of nanoporous alumina membranes is advantageous owing to the large surface area and the light guiding.[54] Moreover, we speculate that coupling of the wave-guiding phenomenon suggested herein with traditional hot-spot design might increase the enhancement factor further by several orders of magnitude and allow the detection of only a few molecules, a phenomenon demonstrated only for few resonance-enhanced Raman markers.[5,6] This design will open a new framework for the fabrication of robust, cost-effective, large-area, ultrasensitive SERS-based sensors for the trace-level detection of nonresonant chemicals and biomolecules, as will be discussed in forthcoming publications.

Experimental Section

Au nanoparticles (32 nm in diameter) capped with cetyltrimethylammonium bromide (CTAB) were prepared by a seed-growth method following a procedure described in the literature.[58] Porous alumina membranes were purchased from Whatman (Anodisc 47); the average pore size was (243 ± 20) nm with 60 μm thickness. The nanoparticles were immobilized on the porous alumina membranes by a modification of a procedure described in the literature.[59] Typically, the inner surface of the porous membranes were modified with PDDA ($M_w = 60{,}000$, Aldrich) by spin-coating of a 0.2% aqueous solution followed by rinsing. Finally, 10 μL of a solution of 2,4-DNT (Aldrich) in ethanol was drop-evaporated on the SERS substrate with an area of 1 cm^2. Field-emission scanning electron microscopy (FESEM, LEO 1530) was used to investigate the assembled structures of decorated membranes. The Raman spectra were recorded by using a Holoprobe Raman microscope (Kaiser Optical Systems) with 10× objective (NA = 0.25) and back-scattered configuration. The excitation laser is a diode laser with 785 nm and the power to the sample is 20 mW.

Keywords:

gold · nanoparticles · nanoporous materials · SERS

[1] G. A. Baker, D. S. Moore, *Anal. Bioanal. Chem.* **2005**, *382*, 1751.
[2] K. Kneipp, H. Kneipp, L. Itzkan, R. R. Dasari, M. S. Feld, *Chem. Rev.* **1999**, *99*, 2957.
[3] D. A. Genov, A. K. Sarychev, V. M. Shalaev, A. Wei, *Nano Lett.* **2004**, *4*, 153.
[4] K. Imura, H. Okamoto, M. K. Hossain, M. Kitajima, *Nano Lett.* **2006**, *6*, 2173.
[5] S. M. Nie, S. R. Emory, *Science* **1997**, *275*, 1102.
[6] K. Kneipp, Y. Wang, H. Kneipp, L. T. Perelman, I. Itzkan, R. R. Dasari, M. S. Feld, *Phys. Rev. Lett.* **1997**, *78*, 1667.
[7] R. Gunawidjaja, S. Peleshanko, H. Ko, V. V. Tsukruk, *Adv. Mater.* **2008**, *20*, 1544.
[8] J. M. Sylvia, J. A. Janni, J. D. Klein, K. M. Spencer, *Anal. Chem.* **2000**, *72*, 5834.
[9] A. Tao, F. Kim, C. Hess, J. Goldberger, R. He, Y. Sun, Y. Xia, P. Yang, *Nano Lett.* **2003**, *3*, 1229.
[10] C. L. Haynes, C. R. Yonzon, X. Y. Zhang, R. P. Van Duyne, *J. Raman Spectrosc.* **2005**, *36*, 471.
[11] E. Anastassakis, A. Pinczuk, E. Burstein, F. H. Pollack, M. Cardona, *Solid State Commun.* **1970**, *8*, 133.
[12] I. De Wolf, *Semicond. Sci. Technol.* **1996**, *11*, 139.
[13] C. Jiang, W. Y. Lio, V. V. Tsukruk, *Phys. Rev. Lett.* **2005**, *95*, 115503.
[14] H. Ko, Y. Pikus, C. Jiang, A. Jauss, O. Hollricher, V. V. Tsukruk, *Appl. Phys. Lett.* **2004**, *85*, 2598.
[15] H. Ko, C. Jiang, H. Shulha, V. V. Tsukruk, *Chem. Mater.* **2005**, *17*, 2490.
[16] C. Jiang, H. Ko, V. V. Tsukruk, *Adv. Mater.* **2005**, *17*, 212.
[17] L. G. Olson, R. H. Uibel, J. M. Harris, *Appl. Spectrosc.* **2004**, *58*, 1394.
[18] M. Fleischmann, P. J. Hendra, A. J. McQuillan, *Chem. Phys. Lett.* **1974**, *26*, 163.
[19] E. L. Torres, J. D. Winefordner, *Anal. Chem.* **1987**, *59*, 1626.
[20] R. G. Freeman, K. C. Grabar, K. J. Allison, R. M. Bright, J. A. Davis, A. P. Guthrie, M. B. Hommer, M. A. Jackson, P. C. Smith, D. G. Walter, M. J. Natan, *Science* **1995**, *267*, 1629.
[21] Z. Wang, S. Pan, T. D. Krauss, H. Du, L. J. Rothberg, *Proc. Natl. Acad. Sci. USA* **2003**, *100*, 8638.
[22] M. Schierhorn, S. J. Lee, S. W. Boettcher, G. D. Stucky, M. Moskovits, *Adv. Mater.* **2006**, *18*, 2829.
[23] T. R. Jensen, G. C. Schatz, R. P. Van Duyne, *J. Phys. Chem. B* **1999**, *103*, 2394.
[24] N. Felidj, J. Aubard, G. Levi, J. R. Krenn, A. Hohenau, G. Schider, A. Leitner, F. R. Aussenegg, *Appl. Phys. Lett.* **2003**, *82*, 3095.
[25] H. Wang, C. S. Levin, N. J. Halas, *J. Am. Chem. Soc.* **2005**, *127*, 14992.
[26] T. Qiu, X. L. Wu, J. C. Shen, P. K. Chu, *Appl. Phys. Lett.* **2006**, *89*, 131914.
[27] H. Ko, S. Singamaneni, V. V. Tsukruk, *Small*. **2008**, *10*, 1576.
[28] M. J. Natan, *Faraday Discuss.* **2006**, *132*, 321.
[29] S. Chan, S. Kwon, T. W. Koo, L. P. Lee, A. A. Berlin, *Adv. Mater.* **2003**, *15*, 1595.
[30] T. L. Williamson, X. Guo, A. Zukoski, A. Sood, D. J. Diaz, P. W. Bohn, *J. Phys. Chem. B* **2005**, *109*, 20186.
[31] J. J. Laserna, W. S. Sutherland, J. D. Winefordner, *Anal. Chim. Acta* **1990**, *237*, 439.
[32] W. S. Sutherland, J. D. Winefordner, *J. Colloid Interface Sci.* **1992**, *148*, 129.
[33] S. J. Lee, Z. Guan, H. Xu, M. Moskovits, *J. Phys. Chem. C.* **2007**, *111*, 17985.
[34] P. M. Tessier, O. D. Velev, A. T. Kalambur, J. F. Rabolt, A. M. Lenhoff, E. W. Kaler, *J. Am. Chem. Soc.* **2000**, *122*, 9554.
[35] L. Lu, A. Eychmuller, A. Kobayashi, Y. Hirano, K. Yoshida, Y. Kikkawa, K. Tawa, Y. Ozaki, *Langmuir* **2006**, *22*, 2605.
[36] L. Qin, S. Zou, C. Xue, A. Atkinson, G. C. Schatz, C. A. Mirkin, *Proc. Natl. Acad. Sci. USA* **2006**, *103*, 13300.
[37] A. G. Brolo, E. Arctander, R. Gordon, B. Leathem, K. L. Kavanagh, *Nano Lett.* **2004**, *4*, 2015.

[38] J. T. Bahns, F. Yan, D. Qiu, R. Wang, L. Chen, *Appl. Spectrosc.* **2006**, *60*, 989.
[39] T. W. Ebbesen, H. J. Lezec, H. F. Ghaemi, T. Thio, P. A. Wolff, *Nature* **1998**, *391*, 667.
[40] D. S. Moore, *Rev. Sci. Instrum.* **2004**, *75*, 2499.
[41] M. Saito, M. Shibasaki, S. Nakamura, M. Miyagi, *Opt. Lett.* **1994**, *19*, 710.
[42] K. H. A. Lau, S. Tan, K. Tamada, M. S. Sander, W. Knoll, *J. Phys. Chem. B* **2004**, *108*, 10812.
[43] http://www.d3technologies.co.uk/products/index.html.
[44] F. Thery-Merland, C. Methivier, E. Pasquinet, L. Hairault, C. M. Pradier, *Sens. Actuators B* **2006**, *114*, 223.
[45] C. Jiang, S. Markutsya, V. V. Tsukruk, *Langmuir* **2004**, *20*, 882.
[46] N. Félidj, J. Aubard, G. Lévi, J. R. Krenn, A. Hohenau, A. Leitner, F. R. Aussenegg, *J. Chem. Phys.* **2004**, *120*, 7141.
[47] A. Ouasri, A. Rhandour, C. Dhamelincourt, P. Dhamelincourt, A. Mazzah, *Spectrochim. Acta Part A* **2002**, *58*, 2779.
[48] K. M. Spencer, J. M. Sylvia, J. A. Janni, J. D. Klein, *Proc. SPIE-Int. Soc. Opt. Eng.* **1999**, *3710*, 373.
[49] A. D. McFarland, M. A. Young, J. A. Dieringer, R. P. VanDuyne, *J. Phys. Chem. B* **2005**, *109*, 11279.
[50] J. B. Jackson, N. J. Halas, *Proc. Natl. Acad. Sci. USA* **2004**, *101*, 17930.
[51] F. J. García-Vidal, J. B. Pendry, *Phys. Rev. Lett.* **1996**, *77*, 1163.
[52] H. H. Wang, C. Y. Liu, S. B. Wu, N. W. Liu, C. Y. Peng, T. H. Chan, C. F. Hsu, J. K. Wang, Y. L. Wang, *Adv. Mater.* **2006**, *18*, 491.
[53] P. K. Jain, W. Y. Huang, M. A. El-Sayed, *Nano Lett.* **2007**, *7*, 2080.
[54] S. V. Gaponenko, *Phys. Rev. B* **2002**, *65*, 140303.
[55] W. Kim, V. P. Safonov, V. M. Shalaev, R. L. Armstrong, *Phys. Rev. Lett.* **1999**, *82*, 4811.
[56] I. M. White, H. Oveys, X. Fan, *Spectroscopy* **2006**, *21*, 36.
[57] D. J. Sirbuly, A. Tao, M. Law, R. Fan, P. Yang, *Adv. Mater.* **2007**, *19*, 61.
[58] K. Kwon, K. Y. Lee, Y. W. Lee, M. Kim, J. Heo, S. J. Ahn, S. W. Han, *J. Phys. Chem. C* **2007**, *111*, 1161.
[59] M. Lahav, T. Sehayek, A. Vaskevich, I. Rubinstein, *Angew. Chem. Int. Ed.* **2003**, *42*, 5575.

Published online: October 15, 2008

